JOURNAL OF PROPULSION AND POWER
Vol. 22, No. 1, January–February 2006

Technical Notes

TECHNICAL NOTES are short manuscripts describing new developments or important results of a preliminary nature. These Notes should not exceed 2500 words (where a figure or table counts as 200 words). Following informal review by the Editors, they may be published within a few months of the date of receipt. Style requirements are the same as for regular contributions (see inside back cover).

Low-Frequency Combustion Oscillations in a Swirl Burner/Furnace

Victor M. Rodriguez-Martinez*
Cardiff University,
The Parade, Cardiff, Wales CF24 0YF, United Kingdom
James R. Dawson†
University of Cambridge,
Cambridge, England CB2 1PZ, United Kingdom
and
Timothy O'Doherty‡ and Nickolas Syred§
Cardiff University,
The Parade, Cardiff, Wales CF24 0YF, United Kingdom

I. Introduction

COMBUSTION instability is one of the most problematic issues surrounding modern combustor development, particularly in gas turbine combustors. The excitation of unsteady pressure oscillations result through organized interaction between periodic heat release and the local unsteady flow in the combustor. Numerous investigations into the mechanisms and effects of combustion instability have been carried out in a variety of combustion systems.[1–7] Although burners are currently being designed to burn fuel lean to achieve good emissions performance, the occurrence of combustion instability is certainly not limited to fuel lean or fully premixed systems. With the exception of pressure gain combustion, the prevalent view is that combustion oscillations hinder the operational range of combustion systems and can ultimately result in component failure. As a consequence, significant research efforts are focusing on the control of combustion instabilities.[8–10]

Only a few articles discussing low-frequency combustion instabilities can be found in the literature[11–13] and they have generally attracted less attention than the higher frequencies associated with the hot-gas volume of the combustor. Even fewer articles are available providing quantitative velocity data in any part of the resonant geometry.[9,10] The term low-frequency used in here refers to frequency ranges of 30–100 Hz with unsteady pressure amplitudes that are greater than 5% of the mean pressure. These instabilities result from excitation of the longitudinal modes of the air supply ducting, form the dominant acoustic geometry of the system, and can exhibit many similarities to those found in pulse combustors, dump combustors, and gas turbine rumble conditions where the flame dynamics are strongly coupled to upstream modulations in airflow. The influence of flow modulations in generating variations in equivalence ratio are a frequently cited mechanism despite that very little quantitative data on the upstream flowfield are available outside the field of pulse combustion.[14] When exited, upstream flow modulations can unite several parts of the geometry into a single mode, excite compound modes, or a convective–acoustic mode.[3,6,9,10,13]

This Technical Note documents the quantitative measurements in the approach flow of self-excited combustion oscillations from confined swirl flames under partially premixed conditions. The instability corresponded to the longitudinal mode(s) of the whole combustion facility with the amplitude of the unsteady pressure great enough to cause periodic flow reversal. The presence of flow reversal distinguishes this work over other recent studies.[9] A simple one-dimensional numerical model was used to verify the oscillation modes. The focus of the work was to investigate the impact of excited modes on the approach flow characteristics by means of cycle resolved velocity and turbulence measurements. The long wavelengths of the instability are unique to the existing literature on combustion instabilities because the spatial trends of the unsteady velocity field and turbulence spectra were ascertained due to the presence of more than one pressure node. Comparison is drawn with turbulence spectra obtained for steady cold-flow conditions.

II. Test Rig

The confined swirling flames were generated by a simple two tangential entry burner and confined in a combustor. The test rig was manufactured from stainless steel and comprised a cylindrical burner section with a 4:1 (area ratio) expansion into a cylindrical furnace section of 150 mm in diameter. The test rig was operated at atmospheric pressure, supplied by natural gas, and was mounted in an upright position. For these experiments a single tangential inlet was employed to simplify the inlet geometry. A flexible duct was fitted to the tangential inlet and was connected to a blower. Three inlet ducts were investigated having lengths of 3.1, 5.9, and 9 m, which, when normalized against the burner exit diameter D_e, give nondimensional total lengths of $l_i/D_e = 42$, 79, and 120. This Note is focused on the $l_i/D_e = 79$ case, although references to the other three lengths are made. The burner could be operated in either a diffusion mode with fuel injection along the centerline or in a premixed mode by injecting natural gas through a fuel bar in the tangential inlet $-3.6D_e$ upstream of the burner plenum. The fuel bar consisted of small orifices drilled into a pipe that injected natural gas in counterflow to the oncoming turbulent air. Both the air and fuel flows were metered with adjustable rotameters. The swirl-stabilized flame formed a V flame that was positioned in and above the burner exit and fired into the combustor. The combustor exit area was modified to excite the instabilities. The rig arrangement is shown in Fig. 1, where all dimensions are in millimeters. The isometric view in Fig. 1a shows the tangential inlet where the variable length air supply ducts were connected.

Depending on the equivalence ratio and the open area at the combustor exit, unsteady pressure amplitudes p'_{amp} ranged from 3.5 to 12 kPa corresponding to 3.5–12% of the mean combustor pressure.

Presented as Paper 2004-811 at the AIAA 42nd Aerospace Sciences Meeting and Exhibit, Reno, NV, 5–8 January 2004; received 6 July 2004; revision received 9 June 2005; accepted for publication 16 June 2005.

*Graduate Student, P.O. Box 925, Institute of Sustainability, Energy and Environmental Management, Cardiff School of Engineering.

†Research Associate, Department of Engineering, Trumpington Street, Cambridge. Member AIAA.

‡Reader, P.O. Box 925, Institute of Sustainability, Energy and Environmental Management, Cardiff School of Engineering.

§Professor, P.O. Box 925, Institute of Sustainability, Energy and Environmental Management, Cardiff School of Engineering. Member AIAA.

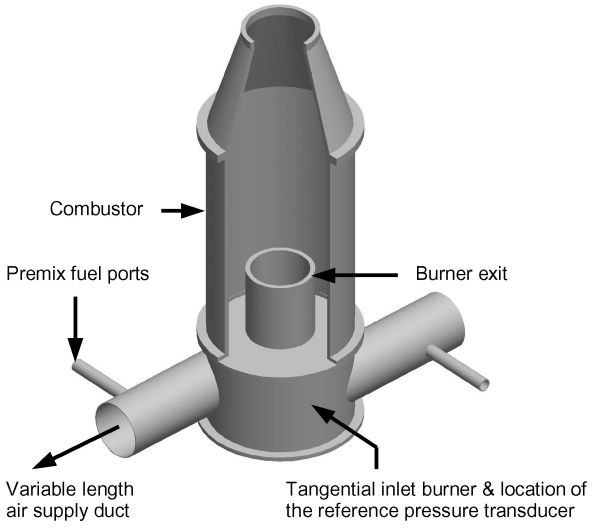

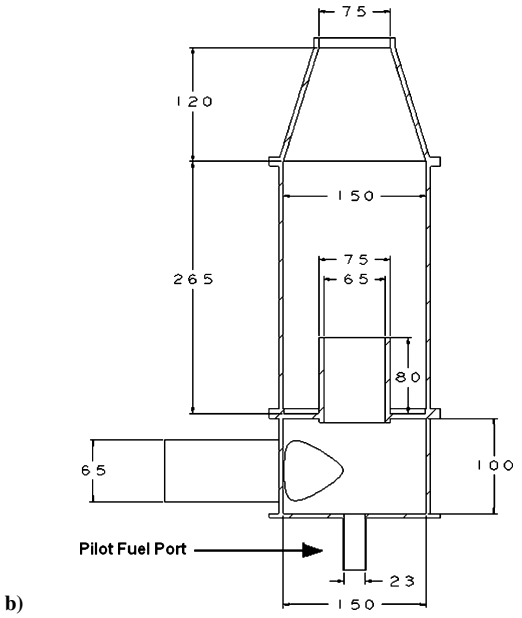

Fig. 1 Test rig: a) isometric view and b) schematic.

The measurements were conducted with $\phi = 0.82$, a total volume flowrate $Q_t = 2380$ l/min with 60% of the fuel injected through the diffusion port and 40% through the premixing fuel bar. This gave an instability frequency of 51 Hz. Although instabilities could be excited for leaner mixtures, the most repeatable instability settings were used to obtain reliable velocity measurements.

III. Pressure and Velocity Measurements

PCB piezoelectric dynamic pressure transducers were placed at different locations across the system to measure the unsteady pressure amplitudes and determine the mode shape. Two pressure transducers were used, one acting as the reference signal positioned at the burner wall, with the other traversed along the inlet. The transducers were charge amplified and monitored online using a two-channel real time digital instruments (DI) 2200 fast Fourier transform analyzer capable of data storage. To quantify the effect of the oscillation on the velocity field of the approach flow, the unsteady pressure signal measured at the burner was used to cycle-resolve velocity measurements that were made using a laser Doppler anemometer (LDA). At each of the measurement positions, the inlet duct was fitted with a transparent section. An isothermal experiment was carried out under the same volumetric flow condition to detect any instability inherent to the cold flow. Only the centerline measurement positions are presented when discussing the inlet flowfield oscillations. The actual locations of both the pressure and velocity measurements are labeled accordingly in the relevant results shown. The LDA system was a Dantec fiber optic laser system with a Coherent Innova 70 series Ar-ion laser with a maximum output of 5 W. The probe lens was set to a focal length of 310 mm with a beam separation of 67 mm. The control volume dimensions of 0.1, 0.1, and 1.3 mm are in x, y, and z coordinates, respectively. Titanium dioxide (TiO_2) seeding was used with a Sauter mean diameter of 1 μm. To cycle resolve the data, the burner pressure signal was bandpass filtered and passed to an oscilloscope to generate a 5V TTL that was used to trigger the LDA system on the zero crossing. There were a minimum of 15,000 validated bursts to ensure statistically accurate data with minimum sampling rates of 0.6 kHz to ensure suitable resolution for obtaining autocorrelations by postprocessing. The velocity data were then resolved into 24 time bins divided over the pressure cycle with each time interval represented by a phase angle from 0 to 360 deg.

IV. Oscillation Characteristics

A typical pressure time series and power spectrums are plotted in Fig. 2 for the longest inlet pipe length $l_i/D_e = 120$. Comparing unsteady pressures p' at the burner and along the inlet duct gives

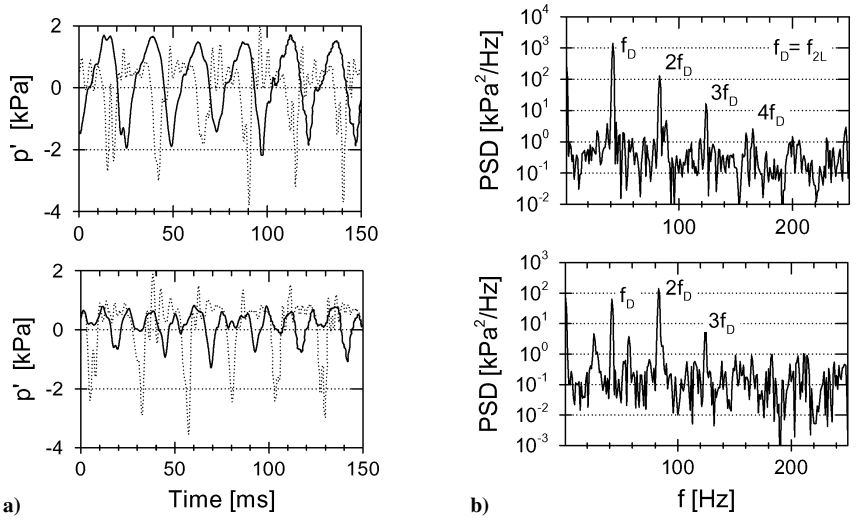

Fig. 2 Simultaneous a) unsteady pressure, $x/D_e = -32.2$ (top) and -55.6 (bottom) and their PSD; ——, different locations along the air inlet referenced to · · · ·, burner wall.

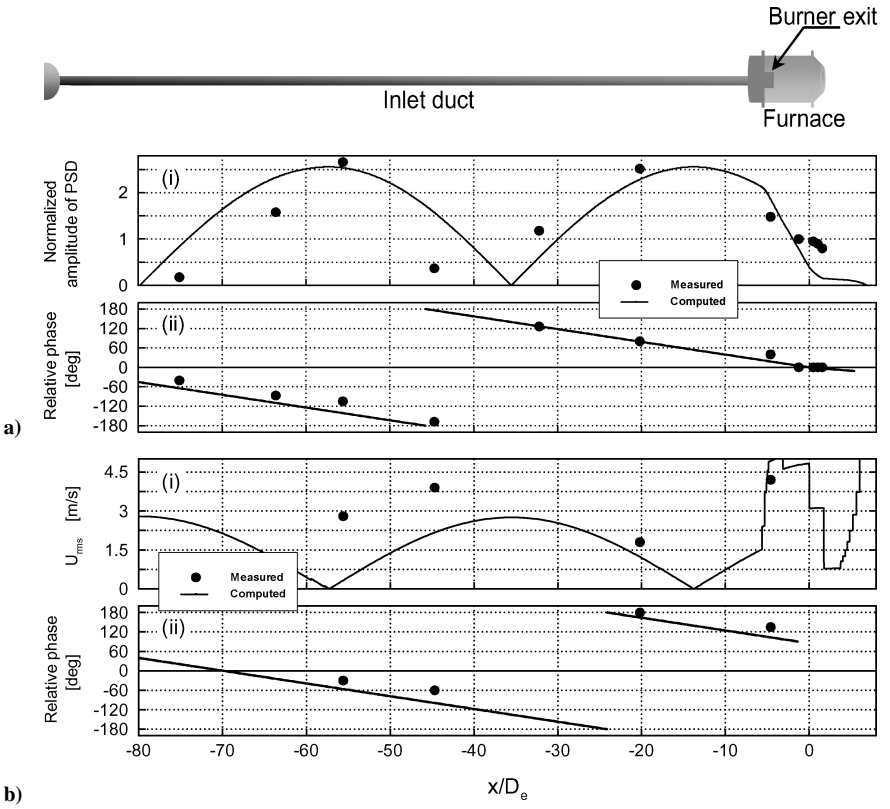

Fig. 3 Measured and predicted velocity mode structure of the pressure oscillation for $l_i/d_e = 79$; 1) unsteady pressure amplitude p' and 2) phase Φ of acoustic pressure: a) amplitude distribution and phase of unsteady pressure p' and b) velocity amplitude distribution $u'_{\rm rms}$ and phase Φ.

a visual indication of the spatial variation in amplitude and phase change. The time-series data for this configuration exhibit an oscillation frequency $f_D = 41$ Hz, with an amplitude distribution corresponding to the $2L$ mode, but the overall trends in phase and spectral content are similar for each inlet length. The amplitude of p' at $x/D_e = -32.2$ is in the vicinity of a pressure antinode, whereas farther upstream at $x/D_e = -55.6$, the measurement location is in the vicinity pressure node.[15] The negative signs denote upstream locations of the burner central axis. Evidence of traveling components illustrate that the wave motion is not purely stationary. The frequency spectrums also reveal some interesting features. Near the pressure antinode at $x/D_e = -32.2$, the power of the resonant frequency f_D is an order of magnitude greater than at $x/D_e = -55.6$. Furthermore, the second harmonic, $2f_D$ at $x/D_e = -55.6$, is greater in magnitude than f_D and is manifested in the increased harmonic response of the pressure time series at this location. The power spectral density (PSD) is shown in Fig. 2b. Overall, the power spectra show that the harmonic response decreases with increasing upstream distance.

A simple one-dimensional modal analysis was conducted to compare with the experimental results and verify the oscillation modes for each of the three inlet configurations. A full description of the acoustic model and detailed analysis for all three inlet lengths is described elsewhere.[7,15] However, a brief discussion follows comparing the measured and predicted phase of unsteady pressure and velocity modes for $l_i/D_e = 79$, as shown in Fig. 3. The resulting instability corresponds to the $2L$ or full-wave mode with three pressure nodes: one at the upstream end of the inlet section, one at approximately half-distance, and a third at the combustor exit. As expected, the locations of velocity antinodes correspond to the positions of the pressure nodes. Despite evidence of traveling components, comparison of the pressure and velocity phases shows that the velocity lags the pressure by approximately one-quarter of the cycle, which indicative of standing waves. It is actually proper to consider the system as pair of opposing traveling waves. Note that for the longest inlet length also excited the $2L$ mode but the shortest inlet length of $l_i/D_e = 42$ excited the $1L$ mode with the unsteady pressure amplitude greater than three times the $2L$ modes of $l_i/D_e = 79$ and 120.

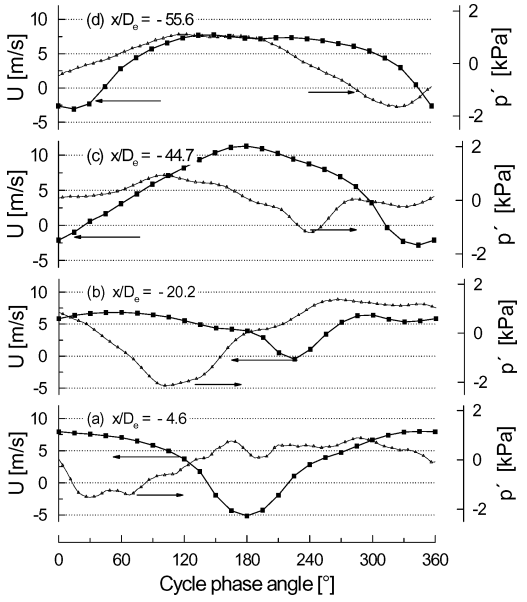

Fig. 4 Cycle-resolved centerline velocities at four axial locations along inlet duct for $l_i/D_e = 79$, $f_D = 51$ Hz and measured p' at each position.

V. Cycle-Resolved Velocities

To examine the actual flow dynamics, a single inlet case was chosen to conduct the velocity measurements. The cycle resolved centerline velocities for $l_i/D_e = 79$ are shown in Figs. 4a–4d. Starting with the cycle-resolved velocity data, the most notable feature of each cycle-resolved velocity profile is the periodic flow reversal during the limit cycle. Nearest the burner at $x/D_e = -4.6$, the centerline velocity shows a sinusoidal response and is approximately 90 deg out of phase with the unsteady pressure field with flow reversal occurring between 150 and 220 deg corresponding to 22% of the limit cycle. Peak velocity of $u > 7.5\ \mathrm{ms}^{-1}$ occurs around ambient pressure

at 0/360 deg, with peak reverse velocity of $u = -5$ ms^{-1} occurring half a cycle later at 180 deg. Farther upstream at $x/D_e = -20.2$, only trace amounts of flow reversal are encountered at 225 deg because the flow tends toward stagnation conditions and the peak velocity slightly reduces to $u > 7$ ms^{-1}. This spatial location is in close proximity to a pressure antinode/velocity node so the decrease in velocity amplitude is accompanied by an increase in the unsteady pressure amplitude. Comparing the profiles at $x/D_e = -4.6$ and -20.2 shows that the flow response of the latter is time shifted by approximately 45 deg.

At $x/D_e = -44.7$, the unsteady pressure amplitude decreases to near minimum and flow reversal is reestablished, occurring between 300 and 30 deg or 25% of the limit cycle, an increase in duration of 3% compared to $x/D_e = -4.6$, although the peak reverse velocity is reduced to $u = -2.5$ ms^{-1}. However, the peak flow velocity has increased to $u > 10$ ms^{-1} between 150 and 205 deg. This is a twofold increase in peak forward velocity compared to the preceding upstream position at $x/D_e = -20.2$ because the measurement locations are close to pressure node/velocity antinode.

At the final upstream measurement position at $x/D_e = -55.6$, the unsteady pressure amplitude has increased, reducing the peak velocities to $u < 8$ ms^{-1} and $u = -3$ ms^{-1}. Flow reversal occurs from 345 to 45 deg, corresponding to a duration of 17% of the limit cycle. Although the mode shapes determine the magnitudes of the pressure and velocity fields, the spatial location with respect to the pressure and velocity nodes also governs the duration of the flow reversal over the limit-cycle period. Unfortunately, additional velocity measurements were not carried out upstream of $x/D_e = -55.6$ to confirm the trend experimentally. The general trend shows that the duration of flow reversal over the limit-cycle period increases when approaching to the pressure node, that is, during the decreasing (favorable) pressure gradient, and decreases toward stagnation approaching the pressure antinode, that is, during the increasing (adverse) pressure gradient.

VI. Velocity Spectra

To investigate the effect of low-frequency combustion oscillations on the turbulence of the approaching airflow, velocity derived autospectral density functions $S(f)$ were obtained to compare with the baseline turbulence spectrum measured under steady cold-flow conditions for the same mass flow rate. The spectra were calculated using Dantec's Burstware software version 3.21, and although the irregular sample intervals is problematic, it has the added advantage of eliminating the Nyquist criterion (see Ref. 16). The software employs a sample and hold method that has limitations at frequencies greater then the data rate, as reported in Ref. 17. However, the frequencies of interest are much lower than the data rates, in fact the lowest data rate of 0.8 kHz is 20 times the fundamental frequency of 41 Hz. Furthermore, the discussion focuses on the relative magnitudes as opposed the absolute magnitudes of the power across the frequency range. Obtaining the spectral content enables comparison of the effect the acoustic oscillations have on the turbulent kinetic energy production with those under steady cold-flow conditions. Examining the cold flow spectrums (shown in gray, Fig. 5) shows the absence of any inherent instability. At low frequency, that is, low wave numbers, the power spectrum remains constant at 10^{-2} m^{2}s^{-1} at all measurement locations along the inlet length, indicative of fully developed turbulent flow. However, when under instability several important features emerge. As expected, discreet high-energy peaks, several orders of magnitude greater than the turbulent energy, are encountered at the instability frequency $f_D = 51$ Hz and associated harmonics of 105, 158, 211, and 265 Hz.

The most significant effects are found by comparing the slope and magnitude of the instability spectra with the cold-flow spectra. Near the pressure node at $x/D_e = -4.6$, the power of the turbulence spectrum increases by an order of magnitude in the low-frequency range and by two orders of magnitude in the fine scales compared to steady flow. Farther upstream near the pressure antinode at $x/D_e = -20.2$, the power of the low-frequency range decreases, tending to the steady flow condition. However, the increase in kinetic energy of the fine-scale turbulence does not decrease with increasing upstream distance and remains at least an order of magnitude greater than the steady cold-flow at all locations. When the pressure node at $x/D_e = -44.7$ is approached, the production of turbulent energy follows the trend encountered at $x/D_e = -4.6$; likewise, the farthest upstream position the energy of the low-frequency turbulence follows the trend encountered at $x/D_e = -20.2$. Clearly the temporal gradients introduced by the unsteady velocity field undergoing flow reversal are driven by the acoustic mode. This produces a net increase in the turbulent kinetic energy content at all length scales/wave numbers when compared to the steady cold-flow turbulence. This is most pronounced in the vicinity of the pressure nodes at $x/D_e = -4.6$ and -44.7, that is, when the velocity amplitude and hence the temporal gradients are a maximum. The velocity spectra indicate that the flow–acoustic interaction may affect the turbulent Reynolds number Re_λ and also exhibits a spatial dependency on the mode shape. In general, these results show that combustion instability can have a significant effect on the turbulence structure of the approach flow and hence alter the mixing processes in the burner normally designed to work under stable flow conditions.

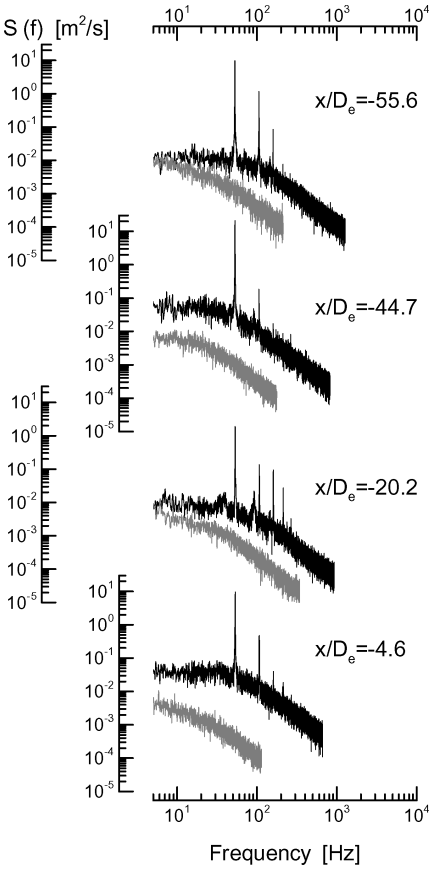

Fig. 5 Power spectrums of centerline velocities in inlet geometry at various upstream positions for $l_i/D_e = 79$, $f_D = 51$ Hz; black, combustion instability and gray, cold-flow conditions respectively.

VII. Conclusions

This Technical Note has examined the effect of naturally excited low-frequency combustion oscillations on the approaching airflow into a partially premixed swirl burner/furnace. The long wavelengths of the instability were used as a platform to obtain cycle-resolved velocity measurements and turbulence spectra along the mode shape to establish the flow modulation characteristics and the effect on the turbulence generation resulting from high-amplitude unsteady pressure oscillations. The main results were as follows.

1) The low-frequency oscillation corresponded to the $2L$ longitudinal mode of the combustion facility with unsteady pressure amplitudes in the order of 10% the mean pressure. As a result, the acoustic mode drove the unsteady velocity gradients, causing flow reversal.

2) Cycle-resolved velocity measurements measured the periodic flow response showing that flow reversal occurs at large upstream distances, beyond $-55.6D_e$. The duration and magnitude of the flow reversal exhibit a spatial dependence on the mode shape. Maximum flow reversal occurs when approaching pressure nodes lasting for 25% of the limit cycle. Periodic reverse flow does not occur at the pressure antinodes, but rather tends to a periodic stagnation.

3) The power spectrum of the turbulence cascade show discreet, high-energy peaks at the resonance frequency and its harmonics throughout the whole inlet geometry. The acoustic–flow coupling produces a net increase in the turbulent kinetic energy at all length scales/wave numbers when compared to the steady cold-flow turbulence, particularly in the vicinity of the pressure nodes where the velocity amplitude and hence the temporal gradients are a maximum.

References

[1]Samaniego, J. M., Yip, B., Poinsot, T., and Candel, S., "Low-Frequency Combustion Instability Mechanisms in a Side-Dump Combustor," *Combustion and Flame*, Vol. 94, No. 4, 1993, pp. 363–380.

[2]Keller, J. O., Bramlette, T. T., Westbrook, C. K., and Dec, J. E., "Pulse Combustion: The Quantification of Characteristic Times," *Combustion and Flame*, Vol. 79, No. 2, 1990, pp. 151–161.

[3]Lee, S.-Y., Seo, S., Broda, J. C., Pal, S., and Santoro, R. J., "An Experimental Estimation of Mean Reaction Rate and Flame Structure During Combustion Instability in a Lean Premixed Gas Turbine Combustor," *Proceedings of the Combustion Institute*, Vol. 28, 2000, pp. 775–782.

[4]Paschereit, C. O., Gutmark, E., and Weisenstein, W., "Excitation of Thermoacoustic Instabilities by Interaction of Acoustics and Unstable Swirling Flow," *AIAA Journal*, Vol. 38, No. 6, 2000, pp. 1025–1034.

[5]Giezendanner, R., Keck, O., Weigand, P., Meier, W., Meier, U., Stricker, W., and Aigner, M., "Periodic Combustion Instabilities in a Swirl Burner Studied by Phase-Locked Planar Laser-Induced Fluorescence," *Combustion Science and Technology*, Vol. 175, 2003, pp. 721–741.

[6]De Zilwa, S. R. N., Uhm, J. H., and Whitelaw, J. H., "Combustion Oscillations Close to the Lean Flammability Limit," *Combustion Science and Technology*, Vol. 160, 2000, pp. 231–258.

[7]Poinsot, T. J., Trouve, A. C., Veynante, D. P., Candel, S. M., and Esposito, E. J., "Vortex-Driven Acoustically Coupled Combustion Instabilities," *Journal of Fluid Mechanics*, Vol. 177, 1987, pp. 265–292.

[8]Yu, K. H., Wilson, K. J., and Schadow, K. C., "Liquid-Fueled Active Instability Suppression," *Proceedings of the Combustion Institute*, Vol. 27, 1998, pp. 2039–2046.

[9]Uhm, J. H., and Acharya, S., "Control of Combustion Instability with a High-Momentum Air-Jet," *Combustion and Flame*, Vol. 139, No. 1–2, 2004, pp. 106–125.

[10]Acharya, S., Murugappan, S., O'Donnell, M., and Gutmark, E. J., "Characteristics and Control of Combustion Instabilities in a Swirl-Stabilized Spray Combustor," *Journal of Propulsion and Power*, Vol. 19, No. 3, 2003, pp. 484–496.

[11]Putnam, A. A., *Combustion-Driven Oscillations in Industry*, American Elsevier, New York, 1971.

[12]Thring, M. W., "Combustion Oscillations in Industrial Combustion Chambers," *Proceedings of the Combustion Institute*, Vol. 12, 1969, pp. 163–168.

[13]Yu, K. H., Trouve, A. C., and Daily, J. W., "Low-Frequency Pressure Oscillations in a Model Ramjet Combustor," *Journal of Fluid Mechanics*, Vol. 232, 1991, pp. 47–71.

[14]Dec, J. E., Keller, J. O., and Hongo, I., "Time-Resolved Velocities and Turbulence in the Oscillating Flow of a Pulse Combustor Tail Pipe," *Combustion and Flame*, Vol. 83, No. 3–4, 1991, pp. 271–292.

[15]Rodriguez-Martinez, V. M., "An Experimental Study of Combustión Instability in Swirl-Stabilized Burner/Furnace Systems," Ph.D. Dissertation, Div. of Mechanical Engineering and Energy Studies, Cardiff Univ., Cardiff, Wales, U.K., 2003.

[16]Britz, D., and Antonia, R. A., "A Comparison of Methods of Computing Power Spectra of LDA Signals," *Measurement Science and Technology*, Vol. 7, 1996, pp. 1042–1053.

[17]Adrian, R. J., and Yao, C. S., "Power Spectra of Fluid Velocities Measured by Laser Doppler Velocimetry," *Experiments in Fluids*, Vol. 5, 1987, pp. 17–28.